

Inhibition Mechanisms of (–)-Epigallocatechin-3-gallate and Genistein on Amyloid-beta 42 Peptide of Alzheimer's Disease via Molecular Simulations

Mei Fang,* Quan Zhang, Xin Wang, Kehe Su, Ping Guan,* and Xiaoling Hu*



Cite This: *ACS Omega* 2022, 7, 19665–19675



Read Online

ACCESS |

Metrics & More

Article Recommendations



ABSTRACT: The misfolding and self-assembly of amyloid-beta ($A\beta$) peptides are one of the most important factors contributing to Alzheimer's disease (AD). This study aims to reveal the inhibition mechanisms of (–)-epigallocatechin-3-gallate (EGCG) and genistein on the conformational changes of $A\beta$ 42 peptides by using molecular docking and molecular dynamics (MD) simulation. The results indicate that both EGCG and genistein have inhibitory effects on the conformational transition of $A\beta$ 42 peptide. EGCG and genistein reduce the ratio of β -sheet secondary structures of $A\beta$ 42 peptide while inducing random coil structures. In terms of hydrophobic interactions in the central hydrophobic core of $A\beta$ 42 peptide, the binding affinities of EGCG are significantly larger in comparison with that of genistein. Our findings illustrate the inhibition mechanisms of EGCG and genistein on the $A\beta$ 42 peptides and prove that EGCG is a very promising inhibitor in impeding the conformational change of $A\beta$ 42 peptide.

INTRODUCTION

Alzheimer's disease (AD), which can cause cognitive functional disorder and behavioral impairment, severely affects the quality of life of the elderly. In most cases, AD has two main pathological features, which are extraneuronal plaques of misfolded amyloid-beta ($A\beta$) proteins and intraneuronal neurofibrillary tangles of hyperphosphorylated tau protein in the brain.¹ Especially, the extracellular $A\beta$ plaques produced by $A\beta$ peptides' aggregation are one of the unique characteristics of AD.² The two main components of $A\beta$ peptides are 40 amino acid residues ($A\beta$ 40 for short) and 42 amino acid residues ($A\beta$ 42 for short). In fact, monomeric $A\beta$ 42 peptide plays a key role in the initial development of $A\beta$ plaques.¹ Oligomers are formed by the self-assembly of misfolded $A\beta$ 42 peptides and then further aggregate to form fibrils. Then

gradually, plaques deposit around nerve cells in the brain (Figure 1).

$A\beta$ 42 monomer is a very important marker of AD, which has been widely used in the prevention and treatment of AD.³ The pathway to prevent the misfolding and further aggregation of monomeric $A\beta$ 42 peptide is either to inhibit conformational transition of $A\beta$ monomer by targeting inhibitors or to stabilize the native state of $A\beta$ 42 monomer by refolding of the misfolded conformation.⁴ As to conformational transition

Received: March 9, 2022

Accepted: May 18, 2022

Published: May 31, 2022



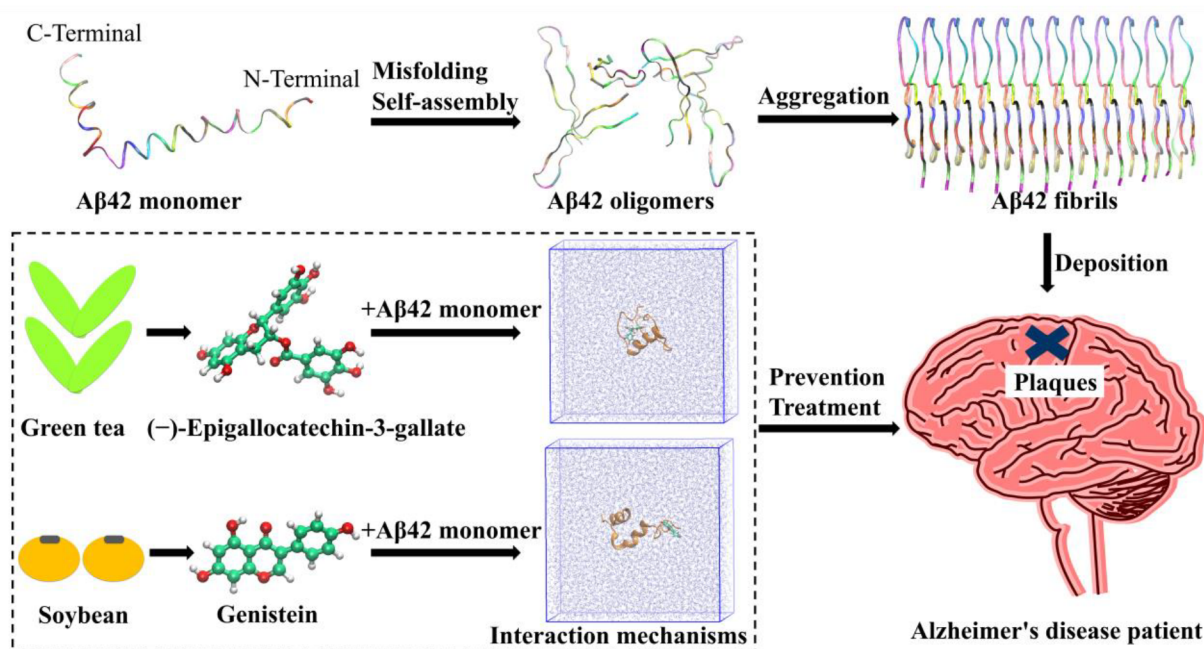


Figure 1. Schematic illustration of possible mechanisms of inhibiting the conformational change of Aβ42 peptide by EGCG and genistein.

inhibitors of Aβ42 monomer, natural polyphenolic compounds extracted from edible plants attract much attention because of their low toxicity and few side effects on the human body.⁵

(-)-Epigallocatechin-3-gallate (EGCG), the major polyphenolic constituent of green tea, has been proven to have a neuroprotective effect on aging and neurodegenerative diseases.^{6,7} Harvey et al. have demonstrated that EGCG is able to disaggregate the preformed Aβ fibrils and protect neuronal cells in vitro.⁸ Similarly, the green tea polyphenol EGCG can redirect the amyloidogenic aggregation pathway by expanding ataxin-3 toward nontoxic, soluble, SDS-resistant aggregates.⁹ Acharya et al. have investigated the molecular mechanisms between EGCG and Aβ polypeptides by combining in vitro immuno-infrared sensor measurements, molecular docking, and molecular dynamics (MD) simulations. They show that the intermolecular interactions of EGCG and Aβ polypeptides are dominated by a few residues in the fibrils.¹⁰ In addition, the interaction mechanisms of EGCG in inhibition of Aβ42 oligomers¹¹ and disaggregation of Aβ42 fibrils^{12,13} have also been studied by using molecular simulations. The results illustrate that EGCG can prevent the aggregation of Aβ42 oligomers and increase the destabilization effect of Aβ42 fibrils.

On the other hand, soybean isoflavone is a typical polyphenol present extensively in soy foods, which has potential therapeutic effects on AD. Ding et al. have found that soybean isoflavones can alleviate the learning and memory deficit induced by Aβ42 peptide in rats by protecting the synapse structure and function.¹⁴ Isoflavones are present in significant quantities in soybeans, which are called genistein (5,7,4'-trihydroxyisoflavone), daidzein (7,4'-dihydroxyisoflavone), and glycitein (7,4'-dihydroxy-6-methoxyisoflavone).¹⁵ Among them, genistein is the main isoflavone, which has the advantage of systemic nontoxicity.¹⁶ Furthermore, genistein not only has an excellent neuroprotective effect but also is a multitarget inhibitor.¹⁷ Ma et al. have demonstrated genistein's neuroprotective effects against Aβ-induced neuroinflammation

through regulating the Toll-like receptor 4/nuclear factor κB signaling pathway.¹⁸ Further, Petry et al. have found that genistein can protect against Aβ-induced toxicity in SH-SY5Y cells by inhibiting Aβ-induced protein kinase B inactivation and tau hyperphosphorylation.¹⁹ Ren et al. have revealed that genistein strongly inhibits Aβ42 monomer self-aggregation at the very beginning of the aggregation. Moreover, MD results showed that genistein prefers to bind the β-sheet groove of Aβ42 pentameric protofibril.²⁰

However, the mechanisms of how the EGCG molecule and genistein molecule inhibit the conformational transitions of Aβ42 monomers have not been well studied at present. In this work, we use molecular simulations to investigate the inhibiting behaviors of EGCG and genistein on the conformational changes of full-length Aβ42 peptides and explore the differences in molecular mechanisms (Figure 1). Meanwhile, the specific binding patterns of EGCG and genistein with Aβ42 peptides are demonstrated by molecular docking simulation. MD simulation studies reveal structural stabilities, secondary structure distributions, and the effect of two polyphenolic molecules on the hydrogen bonds of Aβ42 peptides. In addition, the binding free energy and energy contribution per amino acid residue of Aβ42 peptide in systems with EGCG or genistein are calculated. In conclusion, both EGCG and genistein can inhibit the conformational change of Aβ42 peptide. The differences in the inhibitory mechanisms of EGCG and genistein are also discussed. Our studies provide a theoretical basis for the design of new drug candidates to inhibit the conformational transition and further self-assembly of Aβ42 monomer.

RESULTS AND DISCUSSION

Binding Sites of Aβ42 Monomer. To investigate the specific binding sites of Aβ42 peptide, we adopt the DoGSiteScorer tool to acquire the prediction of binding regions. The binding pockets of Aβ42 monomer are predicted to be pocket 1 (Leu17, Phe20, Ala21, Gly25, Lys28, Ile31,

Ile32, Leu34, and Met35) and pocket 2 (Ser8, Glu11, Val12, Gln15, and Lys16), which are shown in Figure 2. The interaction mechanisms between the two specific binding regions of A β 42 peptide and two polyphenolic molecules are further examined by molecular docking simulation.

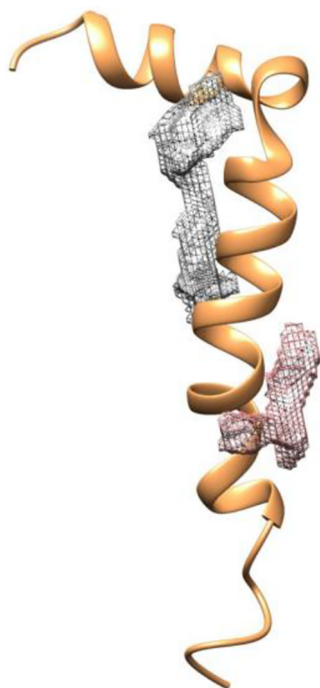


Figure 2. Predicted binding sites of A β 42 peptide: pocket 1 is shown in gray mesh, and pocket 2 is shown in pink mesh.

Molecular Docking Simulation of A β 42 Peptide with Respect to EGCG and Genistein. Autodock can offer information on the interactions of two polyphenolic molecules with the two binding pockets of A β 42 peptide. For interactions between pocket 1 of A β 42 peptide and EGCG, the binding energies are -3.33 kcal/mol and -2.69 kcal/mol for the first and second poses of EGCG, respectively. And the binding energies are -4.28 kcal/mol and -2.85 kcal/mol for the interactions of pocket 2 of A β 42 peptide with the first and second conformations of EGCG. However, only one docking pose of genistein is proposed for the interactions between genistein and pocket 1 of A β 42 peptide. The binding energy is -4.24 kcal/mol. Similarly, only one docking conformation is also obtained between pocket 2 of A β 42 peptide and genistein. The binding energy is -5.10 kcal/mol. Since the negative sign means favorable binding pose,²¹ the lowest values for EGCG (-4.28 kcal/mol) and genistein (-5.10 kcal/mol) illustrate that the conformations of them strongly bind to binding site 2 of A β 42 peptide. Therefore, they are used as optimal candidates. The intermolecular interactions of binding region 2 of A β 42 peptide with the favorable binding conformations of small molecules are considered for further investigations (Figure 3).

As shown in Figure 3a and b, the interactions between the favorable binding pose of EGCG and residues of A β 42 peptide are depicted. The amine group of residue Gln15 is the hydrogen bond donor, and the ester and hydroxyl groups of EGCG are the hydrogen bond acceptors for the hydrogen bonds ($dO\cdots H = 2.09$ Å, $dO\cdots N = 2.99$ Å, $\angle NHO = 147.8^\circ$

and $dO\cdots H = 2.14$ Å, $dO\cdots N = 3.05$ Å, $\angle NHO = 161.1^\circ$). The carboxyl group of residue Asp7 is the hydrogen bond acceptor, and the hydroxyl group of EGCG is the hydrogen bond donor in the hydrogen bond ($dO\cdots H = 2.20$ Å, $dO\cdots O = 3.05$ Å, $\angle OHO = 146.2^\circ$). In addition, hydrophobic interactions between EGCG and residues Asp7, Ser8, Glu11, Val12, Gln15, Lys16, and Phe19 of A β 42 peptide are formed.

Figure 3c and d show that interactions are generated between the optimal binding conformation of genistein and residues of A β 42 peptide. The hydrogen bond ($dO\cdots H = 2.15$ Å, $dO\cdots N = 3.04$ Å, $\angle NHO = 145.9^\circ$) is formed by the amine group of residue Gln15 as the hydrogen bond donor and the carbonyl group of genistein as the hydrogen bond acceptor, and hydrophobic interactions between genistein and residues Ser8, Glu11, Val12, Gln15, Lys16, and Phe19 of A β 42 peptide are formed. Taken together, all of the formed hydrogen bonds are stable according to the literature.²² Both EGCG and genistein have strong interactions with the hydrophobic segment²³ of A β 42 peptide, implying that EGCG and genistein can retard the amyloidogenic potential of monomeric A β 42 peptide.

Molecular Dynamics Simulation of A β 42 Peptide with Respect to EGCG and Genistein. *Validation of Simulation Data.* To verify the MD ensembles of the A β 42 peptide–EGCG system and the A β 42 peptide–genistein system obtained after a 100 ns simulation, the SHIFTX2 program²⁴ has been applied to evaluate the NMR chemical shifts of A β 42 peptides. The correlation coefficients are obtained by calculating the chemical shifts of atoms C α and C β in the A β 42 peptide of the final MD ensembles and the A β 42 peptide used initially for simulation. The NMR chemical shifts of the initial A β 42 peptide are labeled as δ_{exp} , which come from experiments of A β 42 peptide alone carried out in the medium of aqueous solutions of fluorinated alcohols,²⁵ and the NMR chemical shifts of the final A β 42 peptide are labeled as δ_{sim} , which come from one unique generated structure at 100 ns. The final structures of A β 42 peptide at 100 ns differ substantially from the initial configurations, as displayed in Figure 6.

As shown in Figure 4a and b, for the simulation system of A β 42 peptide–EGCG, the correlation coefficients of the chemical shifts of atoms C α and C β are 0.93 and 0.99, respectively. Figure 4c and d shows the correlation coefficients of the A β 42 peptide–genistein system. Similarly, the R values of the chemical shifts of atoms C α and C β are 0.93 and 0.99, respectively. Herein, the high correlation coefficients are consistent with the reports in the literature.^{26,27} The results turn out that the MD ensembles of the systems are reliable with the presence of EGCG and genistein.

Structural Analysis. To examine the stability of the results of MD simulations, the values of the root-mean-square deviation (RMSD) and radius of gyration (Rg) are calculated and the representative trajectories are extracted. As shown in Figure 5a, the RMSD values of three systems achieve stabilities after 70 ns, and the simulation time scale of 100 ns is sufficient to establish stable interactions of the A β 42 peptide with two natural polyphenols. When the systems reach the first metastable states around the starting structures, the RMSD values have stabilized at about 1.27 ± 0.09 nm (A β 42 peptide), 1.23 ± 0.05 nm (A β 42 peptide–EGCG), and 1.13 ± 0.08 nm (A β 42 peptide–genistein). Therefore, the 70–100 ns interval is selected for data collection and further analysis.

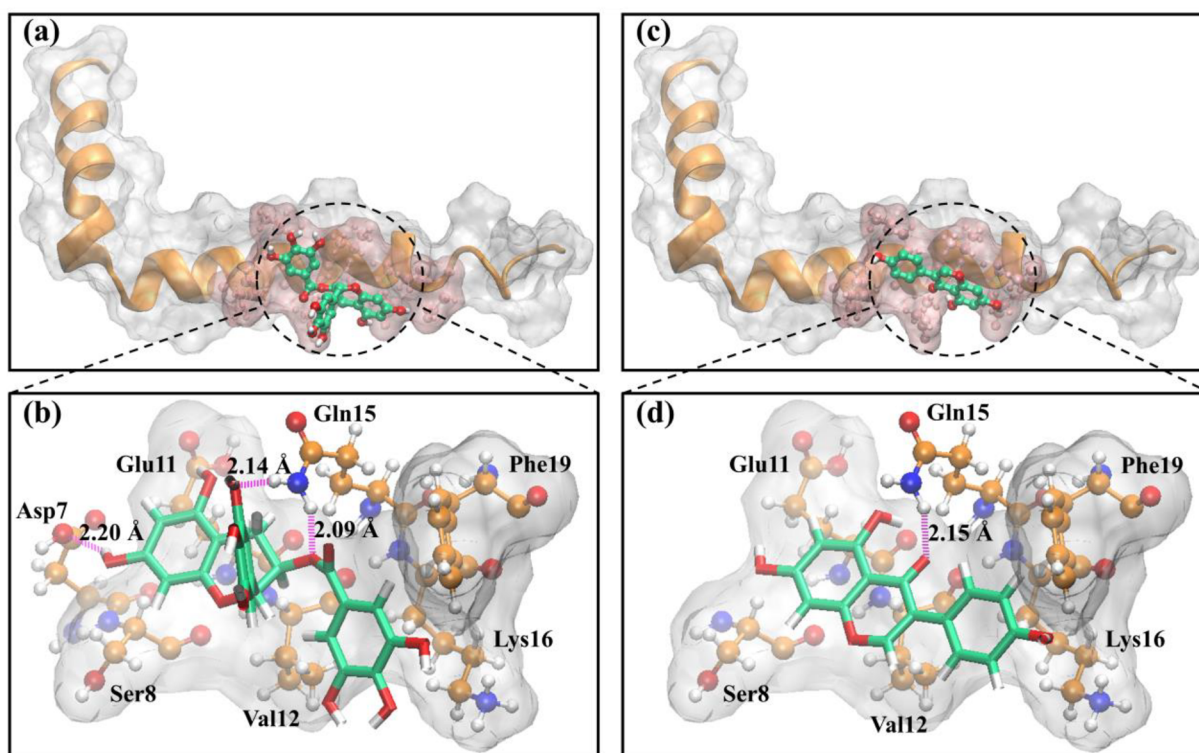


Figure 3. Intermolecular interactions between binding region 2 of Aβ42 peptide and the optimal binding conformations of EGCG and genistein. (a) Aβ42 peptide and EGCG; (b) binding region 2 of Aβ42 peptide and EGCG; (c) Aβ42 peptide and genistein; (d) binding region 2 of Aβ42 peptide and genistein. The hydrogen bonds are shown as purple dotted lines, while the marked residues of Aβ42 peptide make nonbonded contacts with the small molecules.

Figure 5b shows that the values of Rg of the three systems fluctuate greatly within 40 ns and are stabilized at 0.98 ± 0.04 nm (Aβ42 peptide), 1.03 ± 0.05 nm (Aβ42 peptide–EGCG), and 1.04 ± 0.06 nm (Aβ42 peptide–genistein). The results show that the Aβ42 peptides of three systems have undergone great conformational changes in the initial stage of the simulations and then have begun to stabilize after 70 ns. In addition, compared with the Rg value of the control system, the Rg values of the systems (Aβ42 peptide–EGCG and Aβ42 peptide–genistein) are slightly higher, which indicates that the compactness of Aβ42 peptide is reduced and the conformational changes of Aβ42 peptide are affected by the presence of EGCG and genistein.

In addition, representative snapshots of the three systems at different time points have been also compared. As shown in Figure 6a, the configuration of Aβ42 peptide in the control system has changed a lot at the beginning of the simulation trajectory. After the configuration of Aβ42 peptide is stable, β-sheet secondary structures are obviously observed. For the systems Aβ42 peptide–EGCG (Figure 6b) and Aβ42 peptide–genistein (Figure 6c), the configurations of Aβ42 peptide begin to undergo great changes and stretch gradually. After reaching the first metastable states around the starting structures, the secondary structures of Aβ42 peptide influenced by EGCG and genistein are dominated by random coils and α-helical structures. More detailed investigations of the secondary structural changes are discussed in the Secondary Structure Analysis section. Herein, the changing trends of the morphologies of three Aβ42 monomers are shown to be in agreement with those of RMSD and Rg.

In order to further compare the Aβ42 peptide influenced by EGCG and genistein, the values of the root-mean-square fluctuation (RMSF) and solvent accessible surface area (SASA) are examined. The RMSF value indicates the changes of amino acid residues in the Aβ42 peptide chain. As shown in Figure 7a, the fluctuations of amino acid residues in the Aβ42 peptide–EGCG system and the Aβ42 peptide–genistein system are more significant than that in the Aβ42 peptide system. Overall, the central hydrophobic core ($L_{17}VFFA_{21}$)²³ of Aβ42 peptide shows dramatic changes under the influence of EGCG. Compared to EGCG, genistein has a slighter effect on the hydrophobic segment and exhibits a stronger impact on the C-terminus of Aβ42 peptide.

Figure 7b displays the results of the solvent accessibility of the Aβ42 peptide surfaces in different simulation systems. The SASA value is very important for the influence of the configuration of a protein in water.²⁸ It is obvious that the values of SASA have stabilized at about 33.27 ± 1.12 nm²/N (Aβ42 peptide), 35.16 ± 3.10 nm²/N (Aβ42 peptide–EGCG), and 34.37 ± 1.50 nm²/N (Aβ42 peptide–genistein). This result means that the contact areas between the surfaces of Aβ42 peptide and water are increased under the action of EGCG and genistein. The SASA value of the Aβ42 peptide–EGCG system is slightly increased in comparison with that of the Aβ42 peptide–genistein system, implying that Aβ42 peptide can be more exposed to the water molecules in the presence of EGCG.

In sum, by combining RMSD, Rg, RMSF, and SASA data, the results demonstrate that EGCG and genistein show the inhibition of conformational changes against Aβ42 peptides, while the inhibition effect of EGCG on the conformational

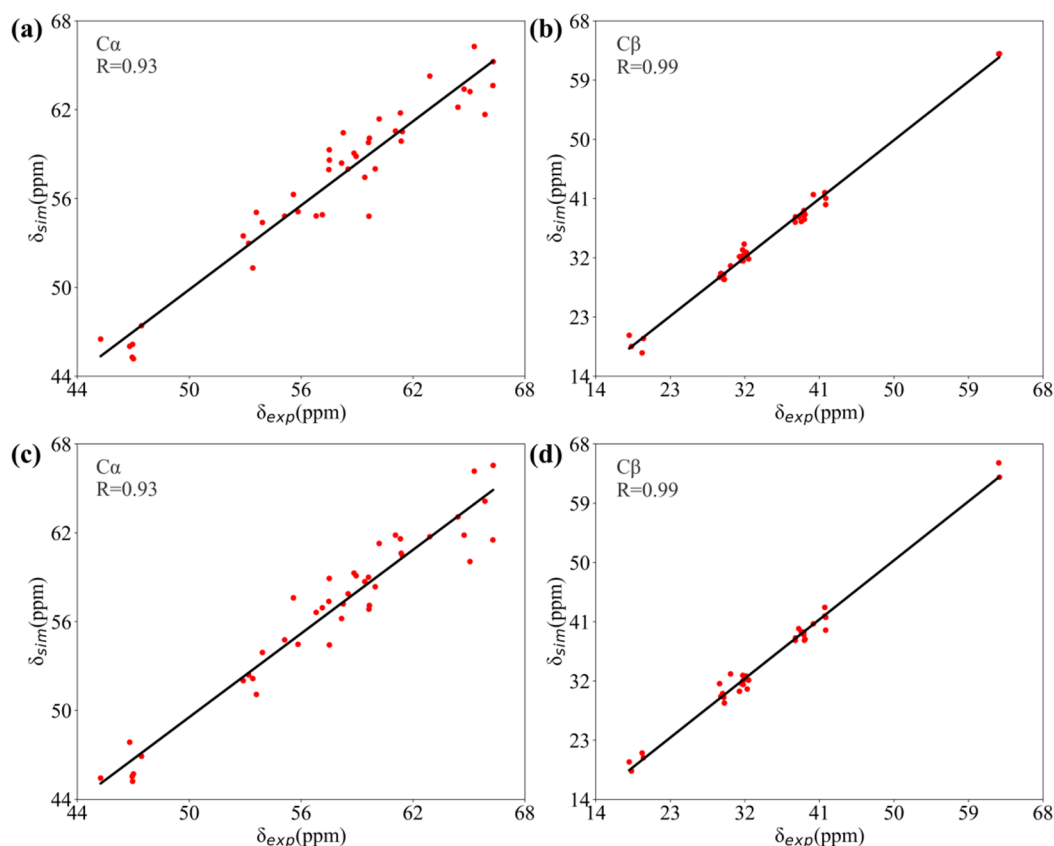


Figure 4. Correlation of the NMR chemical shifts for atoms $C\alpha$ and $C\beta$ between the $A\beta 42$ peptide used initially for simulation and the $A\beta 42$ peptide of the final MD trajectories. (a and b) $A\beta 42$ peptide–EGCG system; (c and d) $A\beta 42$ peptide–genistein system. The unit of the NMR chemical shift is ppm.

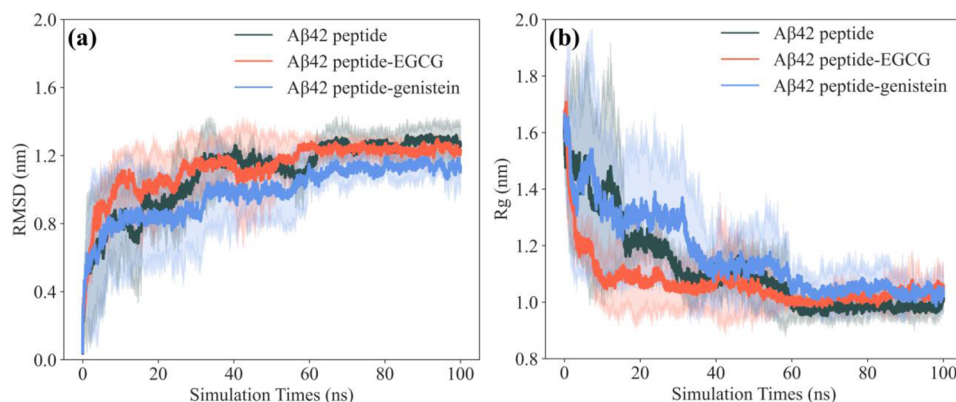


Figure 5. (a) Backbone RMSD of $A\beta 42$ peptide in water and $A\beta 42$ peptide with respect to EGCG and genistein. (b) Total Rg of $A\beta 42$ peptide in water and $A\beta 42$ peptide with respect to EGCG and genistein.

transition of $A\beta 42$ peptide is better than that of genistein. The reason for this could be that the hydrophobic interactions between the EGCG molecule and $A\beta 42$ peptide are stronger. Our findings are also fully similar to those of another simulation study by Li et al., who suggest that EGCG interacts with $A\beta 42$ monomers mainly through hydrophobic interactions and inhibits the formation of $A\beta 42$ dimers.¹²

Secondary Structure Analysis. It has been reported that the conformational conversions of peptide from the initial α -helix to β -sheet are then reorganized into a more organized β -sheet-rich structure, which ultimately leads to $A\beta$ amyloidogenesis.²⁹ To demonstrate how to inhibit the conformational

changes of $A\beta 42$ peptide by EGCG and genistein, the definition of secondary structure of proteins (DSSP) is employed to offer information on the secondary structure contents of $A\beta 42$ peptide in three simulated systems (Table 1). Figure 8b and c displays the time evolution of the secondary structures of $A\beta 42$ peptide in the systems with EGCG and genistein, respectively. Because the balance of helical elements is not produced correctly by the parameter set of the GROMOS force field family,³⁰ the sum of helical structures is marked as the α -helix.³¹

As shown in Table 1 and Figure 8, the proportion of α -helix is 45.28% for the system $A\beta 42$ peptide. The average values of

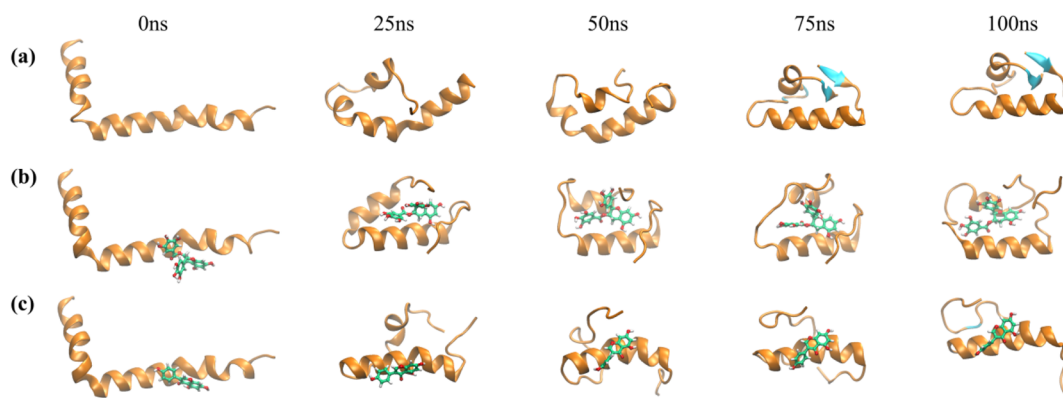


Figure 6. Evolution of configurations of A β 42 peptide (a) in water, (b) with EGCG in water, and (c) with genistein in water. Water molecules are not shown for clarity.

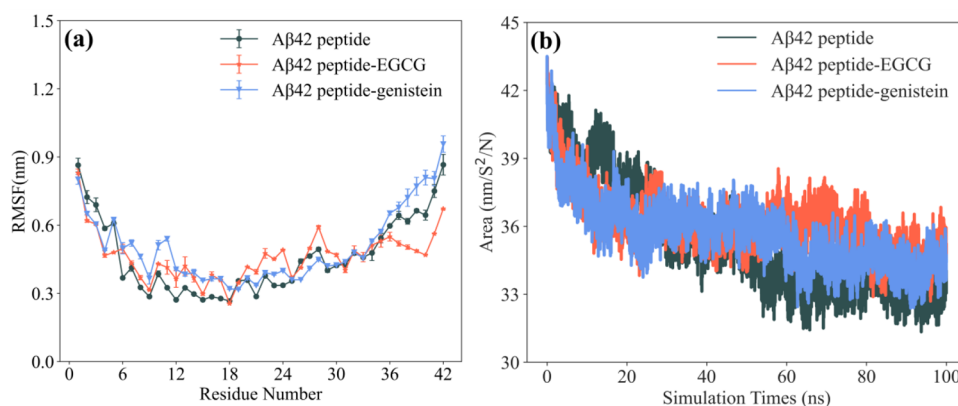


Figure 7. (a) RMSF values for A β 42 peptide in water and A β 42 peptide with respect to EGCG and genistein. (b) SASA values for A β 42 peptide in water and A β 42 peptide with respect to EGCG and genistein.

Table 1. Comparison of Secondary Structure Components in the Systems A β 42 Peptide, A β 42 Peptide–EGCG, and A β 42 Peptide–Genistein

secondary structure component (%)	coil	β -sheet	β -bridge	bend	turn	α -helix ^a
A β 42 peptide	24.69 \pm 4.58	2.75 \pm 1.82	2.45 \pm 0.86	14.91 \pm 4.91	9.92 \pm 6.06	45.28 \pm 2.42
A β 42 peptide–EGCG	28.00 \pm 8.02	0	0.29 \pm 0.05	15.40 \pm 7.93	11.31 \pm 6.94	45.01 \pm 7.44
A β 42 peptide–genistein	29.52 \pm 8.90	0	0.12 \pm 0.02	13.59 \pm 6.89	13.01 \pm 3.95	43.76 \pm 12.85

^aThe 5-helix and 3-helix in Figure 8 correspond to the α -helix.

α -helical structures are 45.01% (A β 42 peptide–EGCG) and 43.76% (A β 42 peptide–genistein). The average helical percentage of A β 42 peptide with the presence of EGCG is only a little less than that in the control system, which shows that the effect of EGCG on the α -helix of A β 42 peptide is not obvious, while genistein can significantly reduce the component ratio of α -helical structures of A β 42 peptide. Moreover, the average percentages of random coils in the A β 42 peptide–EGCG system (28.00%) and the A β 42 peptide–genistein system (29.52%) are markedly increased relative to that in the A β 42 peptide system (24.69%). The proportions of β -sheet structures greatly decrease from 2.75% in the control system to 0 in systems with EGCG and genistein. Taken together, EGCG and genistein can enhance the ratios of random coil structures and especially reduce the content of β -sheet secondary structures. The results indicate that EGCG and genistein can cause structural disorder to A β 42 peptide and have effectively impeded the conformational transitions of A β 42 peptide.

Hydrogen Bond Analysis. In order to further investigate the mechanisms of inhibiting conformational changes of A β 42 peptides by EGCG and genistein, we analyze the effects of two polyphenolic molecules on the hydrogen bonds (H-bonds) of A β 42 peptides. As shown in Figure 9, the average number of H-bonds has stabilized at about 27 \pm 3 (A β 42 peptide), 26 \pm 2 (A β 42 peptide–EGCG), and 25 \pm 4 (A β 42 peptide–genistein). Compared with the H-bond number of A β 42 peptide in the control system, the H-bond break rates of A β 42 peptide are 3.70% (A β 42 peptide–EGCG) and 7.41% (A β 42 peptide–genistein). In other words, the average number of H-bonds has slightly decreased with the existence of EGCG and genistein, respectively, which implies that the intramolecular H-bonds of the peptide chain partially dissociate. Previous studies have shown that the intramolecular H-bonds of A β peptide play a critical role in structural stability and amyloid peptide aggregation.³² Thus, EGCG and genistein show inhibition against conformational changes of A β 42 peptides.

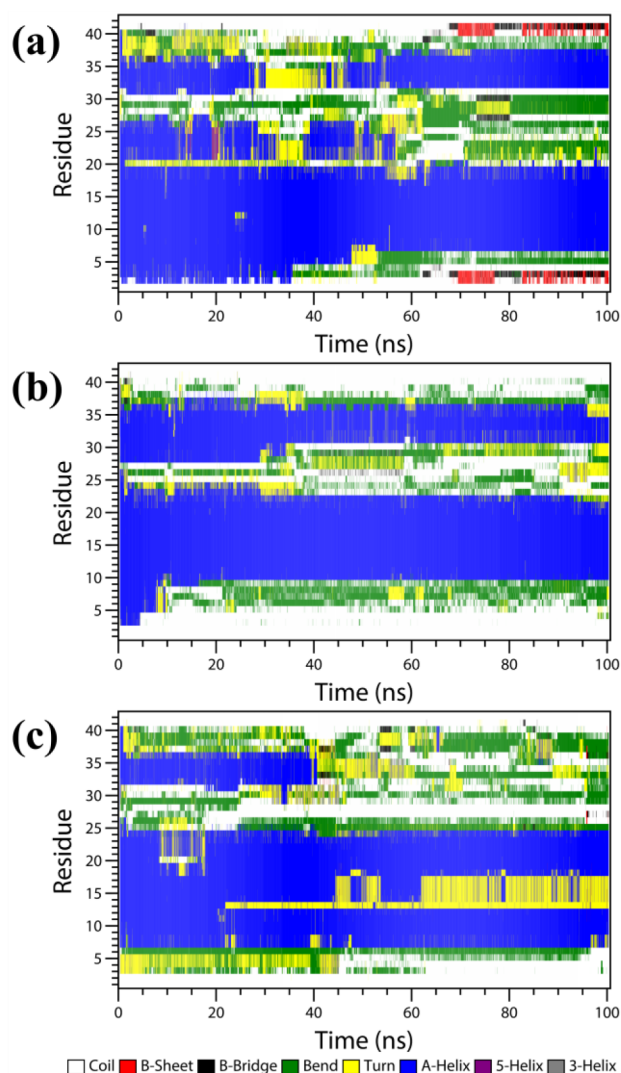


Figure 8. Time evolution of the secondary structures of A β 42 peptide in (a) the A β 42 peptide system, (b) the A β 42 peptide–EGCG system, and (c) the A β 42 peptide–genistein system. The vertical axis represents the residue numbers of A β 42 peptide, and the horizontal axis represents the simulation time in nanoseconds. The secondary structures are color-coded.

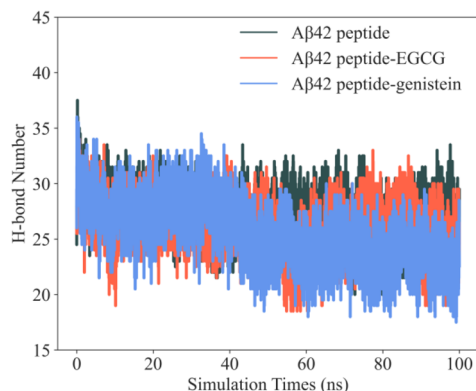


Figure 9. Comparison of the H-bond numbers in A β 42 peptide.

Binding Free Energy Analysis. To further confirm the intermolecular interactions, we have calculated the binding free

energy ($\Delta G_{\text{binding}}$) of A β 42 peptide with respect to EGCG and genistein. The last 30 ns trajectories with $\Delta t = 100$ ps of the A β 42 peptide–EGCG system and the A β 42 peptide–genistein system are collected and calculated by the MM-PBSA method. Various energy terms are depicted in Table 2. The average

Table 2. Various Energy Terms of the Binding Free Energy of A β 42 Peptide with Respect to EGCG and Genistein^a

energy terms	A β 42 peptide–EGCG (kcal/mol)	A β 42 peptide–genistein (kcal/mol)
ΔE_{vdW}	-32.38 ± 8.14	-9.01 ± 3.80
ΔE_{elec}	-14.68 ± 0.21	-41.58 ± 7.53
ΔE_{MM}^b	-47.06 ± 8.11	-50.59 ± 7.90
ΔG_{ps}	30.90 ± 6.03	49.59 ± 8.54
ΔG_{nps}	-3.90 ± 0.72	-2.59 ± 0.27
ΔG_{solv}^c	27.00 ± 5.37	47.00 ± 8.32
$\Delta G_{\text{binding}}^d$	-20.06 ± 4.62	-3.59 ± 0.78

^aThe unit of each energy term is kcal/mol. ^b $\Delta E_{\text{MM}} = \Delta E_{\text{vdW}} + \Delta E_{\text{elec}}$.

^c $\Delta G_{\text{solv}} = \Delta G_{\text{ps}} + \Delta G_{\text{nps}}$. ^d $\Delta G_{\text{binding}} = \Delta E_{\text{MM}} + \Delta G_{\text{solv}}$.

value of $\Delta G_{\text{binding}}$ between the A β 42 peptide and EGCG is about -20.06 ± 4.62 kcal/mol, wherein the molecular mechanics potential energy in a vacuum ($\Delta E_{\text{MM}} = -47.06 \pm 8.11$ kcal/mol), which is favorable for binding, consists of the van der Waals interactions ($\Delta E_{\text{vdW}} = -32.38 \pm 8.14$ kcal/mol) and electrostatic interactions ($\Delta E_{\text{elec}} = -14.68 \pm 0.21$ kcal/mol), while the sum of the polar contribution ($\Delta G_{\text{ps}} = 30.90 \pm 6.03$ kcal/mol) and the nonpolar contribution ($\Delta G_{\text{nps}} = -3.90 \pm 0.72$ kcal/mol) is the Gibbs free energy of solvation ($\Delta G_{\text{solv}} = 27.00 \pm 5.37$ kcal/mol), which is unfavorable for binding. In summary, the van der Waals interactions between the A β 42 peptide and EGCG play an important part in the binding affinities. In other words, the hydrophobic interactions are dominant in the intermolecular energy of A β 42 peptide with EGCG. The results are also consistent with previous studies, which have reported that the nonpolar interactions contribute more than 71% to the binding free energy of the EGCG–A β 42 peptide complex.³¹

However, the average value of $\Delta G_{\text{binding}}$ (-3.59 ± 0.78 kcal/mol) is relatively small for the A β 42 peptide–genistein system. The electrostatic term ($\Delta E_{\text{elec}} = -41.58 \pm 7.53$ kcal/mol) makes an excellent contribution to the binding free energy. While the average value of the van der Waals interactions ($\Delta E_{\text{vdW}} = -9.01 \pm 3.80$ kcal/mol) is small, the average value of ΔG_{nps} is -2.59 ± 0.27 kcal/mol. Compared to other energy terms, the polar term ($\Delta G_{\text{ps}} = 49.59 \pm 8.54$ kcal/mol) is more unfavorable for binding. Therefore, the results suggest that genistein has a weaker interaction with A β 42 peptide than EGCG.

In addition, we have investigated the binding free energy contribution of each residue of A β 42 peptide in the A β 42 peptide–EGCG system and the A β 42 peptide–genistein system. Previous studies have shown that the residues, which contribute less than -1.0 kcal/mol to the binding free energy, are defined as the important residues for binding to ligand.³³ Figure 10a shows the contribution of each residue of A β 42 peptide to the binding free energy in the A β 42 peptide–EGCG system. The residue Phe19 contributes the largest energy to the binding of A β 42 peptide with EGCG. The reason for this could be that the residue Phe19 in the central hydrophobic core has strong hydrophobic interactions with the EGCG molecule, which is in agreement with the reported result.³⁴ As

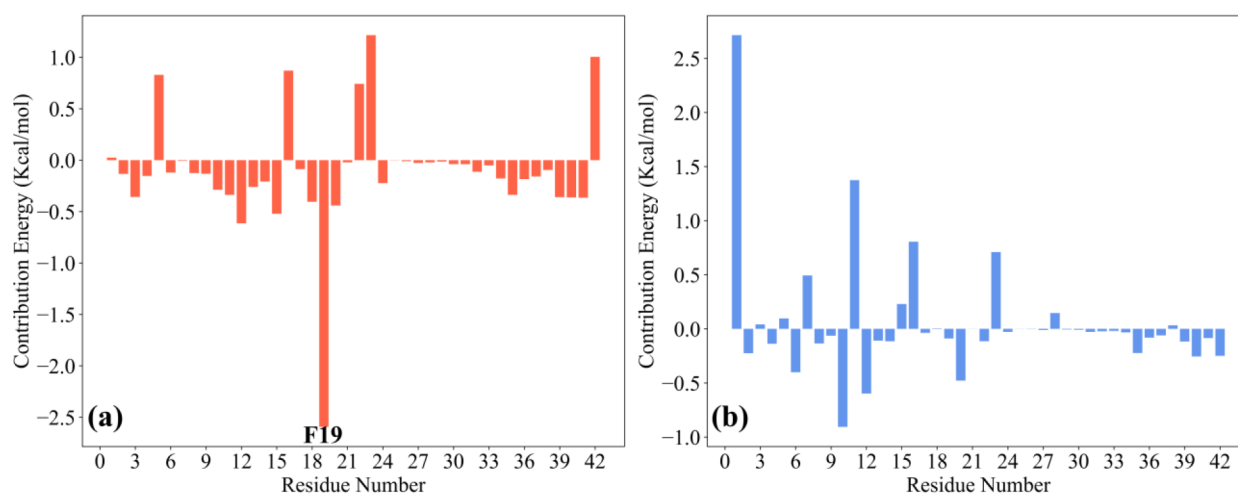


Figure 10. Contribution of each residue of A β 42 peptide to the binding free energy in (a) the A β 42 peptide–EGCG system and (b) the A β 42 peptide–genistein system.

shown in Figure 10b, the binding free energy contribution per residue of A β 42 peptide in the A β 42 peptide–genistein system is above -1.0 kcal/mol, which means that the binding affinity between genistein and A β 42 peptide is low. In sum, the results of binding free energy analysis demonstrate that EGCG can indeed effectively inhibit the conformational transition of A β 42 peptide, while genistein shows less ability to prevent the conformational change of A β 42 peptide.

CONCLUSION

The misfolded conformation of A β 42 peptide plays a dominant role in the initial formation of A β plaques. In this work, we have investigated the effects of EGCG and genistein on the conformational evolution of A β 42 peptide by using molecular docking and MD simulation. The two specific binding regions of A β 42 peptide have been obtained by the DoGSiteScorer tool. The results of the molecular docking simulation show that EGCG and genistein have the optimal binding conformations with binding region 2 of A β 42 peptide. In addition, MD simulation studies illustrate that EGCG and genistein can block the conformational transitions of A β 42 peptides. Compared with the inhibitory effect of genistein, EGCG has stronger intermolecular interactions with A β 42 peptide. The results have also been demonstrated by the MM-PBSA method, indicating that the hydrophobic interactions between EGCG and the central hydrophobic core of A β 42 peptide play an important role in the affinities. Therefore, EGCG is very promising in inhibiting the misfolded conformation and self-assembly of A β 42 peptide.

METHODS

Structure Preparation. The three-dimensional (3D) structure of A β 42 monomer (PDB ID: 1IYT) is obtained from the protein databank (PDB). The sequence of A β 42 peptide is D₁AEFRHDSGYEVHHQKLVFFAEDVGSNKGAIIGLMVGGVVIA₄₂. 1IYT is the 3D NMR structure of A β 42 peptide, which is determined as the full-sized structure comprising residues 1–42 stably and the length and position of two helical regions accurately in the medium of aqueous solutions of fluorinated alcohols.²⁵ Therefore, 1IYT as a topology model is applied to study conformational changes with or without inhibitors.¹¹ In addition, the topologies of

A β 42 monomer populate two distinct states: one is free of secondary structure, and the other has some helical regions, which are determined by the deep learning AlphaFold2 method, and can also be used to help design new inhibitors.³⁵ Model 1 of the NMR conformation in PDB file 1IYT is used for docking and MD simulation. AutoDockTools 1.5.6 software³⁶ is used for the conversion of PDB file formats. The structures of the EGCG molecule (CID: 65064) and genistein molecule (CID: 5280961) are taken from PubChem. The optimizations of the two polyphenols are performed with the Hartree–Fock method with the 6-31G(d) basis set by using Gaussian09W, Revision A.02, software.³⁷ EGCG and genistein are submitted to Automated Topology Builder and Repository version 3.0 (ATB3.0)³⁸ to get the GROMOS96 force field parameters for MD simulation.

Binding Region Prediction. The specific binding sites of A β 42 peptide with natural polyphenolic compounds have not been reported. Therefore, the binding regions of A β 42 peptide are predicted by the DoGSiteScorer tool of ProteinsPlus, which is an online server. DoGSiteScorer can be employed to predict binding sites and estimate druggability.³⁹ A visualization of the binding sites is performed with UCSF Chimera.⁴⁰ Subsequently, binding regions are obtained and used for the following molecular docking simulation.

Molecular Docking Simulation. The AutoDock 4.2 software⁴¹ can be utilized to perform the molecular docking simulations between A β 42 peptide and the two polyphenolic molecules. AutoDock 4.2 is a widely used docking program with exceptional accuracy.⁴² The gasteiger charges and polar hydrogens are added to A β 42 peptide and the two polyphenolic molecules, respectively. A β 42 peptide is selected as a rigid receptor, and small molecules are set as flexible ligands throughout the docking process. The grid box for binding region 1 of A β 42 monomer is set to $54 \text{ \AA} \times 40 \text{ \AA} \times 60 \text{ \AA}$ with the grid center defined as $x = 3.741$, $y = -1.434$, and $z = -5.781$. The grid spacing is 0.375 \AA . The Lamarckian genetic algorithm (LGA) is used for the stochastic search algorithm of docking.⁴³ Specifically, the binding conformations for ligands are generated with the maximum number of energy evaluations (2.5×10^6). All other parameters are left at the default settings.

For the docking between binding region 2 of A β 42 peptide and the two polyphenolic molecules, the setting of each

parameter is quite similar to that of binding region 1, except that the grid box is set to $42 \text{ \AA} \times 42 \text{ \AA} \times 44 \text{ \AA}$ with the grid center defined as $x = -3.775$, $y = -2.583$, and $z = 7.965$. All other arguments are implemented in the same way as those of binding region 1. AutoDockTools 1.5.6 and visual molecular dynamics (VMD) software⁴⁴ are utilized for the analysis and visualization of the results of the docking between the two binding pockets and small molecules. In order to do further study on the interaction mechanisms of the optimal active pockets of A β 42 peptide with the favorable docking conformations of EGCG and genistein, molecular dynamics simulations are performed.

Molecular Dynamics Simulation. GROMACS package 5.1.4⁴⁵ is applied to all MD simulations. First, the models of the A β 42 peptide–EGCG complex and the A β 42 peptide–genistein complex are constructed by the A β 42 peptides and the optimal binding poses of EGCG and genistein. The model of A β 42 peptide in water is used as the control system. The GROMOS96 54a7 force field,⁴⁶ which has reported that the simulation results of A β peptide are consistent with experimental data,⁴⁷ is chosen to model the potential parameters of A β 42 peptide. The protonation states of the N-terminus and C-terminus of A β 42 peptide are assigned according to the physiological pH. Periodic boundary conditions defined in all directions are performed in the $7.28 \times 7.28 \times 7.28 \text{ nm}^3$ cubic box. The SPC water model⁴⁸ is chosen as the water solvent, and three sodium ions as counterions are added to neutralize the negative charges on A β 42 peptide. Specific parameters are listed in Table 3.

Table 3. Specific Parameter Settings of Three System Models

system model	simulation time (ns)	number of total atoms in the simulation box	number of counterions (Na ⁺) in the simulation box
A β 42 peptide	100×3^a	37234	3
A β 42 peptide–EGCG	100×3^a	37258	3
A β 42 peptide–genistein	100×3^a	37246	3

^aMeasurements have been performed three times for each model using different initial velocities.

Second, energy minimization of each system is performed by the steepest descent algorithm. The NVT and NPT ensembles⁴⁹ are adopted to equilibrate the system before measurement. The temperature 300 K and 1 bar pressure are determined by the V-rescale thermostat⁵⁰ and Parrinello–Rahman barostat isotropically.⁵¹ The LINCS algorithm⁵² is utilized to constrain the bonds of A β 42 peptide and the two polyphenolic molecules. The cutoff value of short-range van der Waals interactions is set to 14 Å, and the long-range electrostatic interactions are calculated by the particle mesh Ewald (PME) method.⁵³

In addition, GROMACS provides extremely high performance compared to other programs.⁵⁴ Since the three systems can fully attain the first metastable states around the starting structures within 100 ns MD simulations on the basis of a plateau in the RMSD profile, MD simulations for the systems are monitored for 100 ns with a time step of 2 fs.⁵⁵ To validate the reproducibility and statistical significance of the results,

measurements are performed three times for the three models using different initial velocities, and the data are expressed as average values. The MD trajectories are analyzed and visualized by the tools of GROMACS and VMD. The RMSD is subject to the peptide backbone atoms relative to their initial conformations. The secondary structural data of A β 42 peptide is calculated by the STRIDE algorithm,⁵⁶ and the secondary structural contents are identified by the definition of secondary structure of proteins (DSSP).⁵⁷ The binding free energy and energy contribution per amino acid residue of A β 42 peptide in the systems with EGCG and genistein are calculated by the g_mmpbsa package,⁵⁸ which uses the molecular mechanism Poisson–Boltzmann surface area (MM-PBSA) method⁵⁹ for GROMACS.

AUTHOR INFORMATION

Corresponding Authors

Mei Fang – Department of Chemistry, School of Chemistry and Chemical Engineering, Northwestern Polytechnical University, Xi'an, Shaanxi 710072, China; orcid.org/0000-0002-2754-4572; Email: fangmei@mail.nwpu.edu.cn

Ping Guan – Department of Chemistry, School of Chemistry and Chemical Engineering, Northwestern Polytechnical University, Xi'an, Shaanxi 710072, China; Email: guanping1113@nwpu.edu.cn

Xiaoling Hu – Department of Chemistry, School of Chemistry and Chemical Engineering, Northwestern Polytechnical University, Xi'an, Shaanxi 710072, China; Email: huxl@nwpu.edu.cn

Authors

Quan Zhang – Department of Biomedical Engineering, School of Life Science and Technology, Xi'an Jiaotong University, Xi'an, Shaanxi 710049, China

Xin Wang – Department of Chemistry, School of Chemistry and Chemical Engineering, Northwestern Polytechnical University, Xi'an, Shaanxi 710072, China

Kehe Su – Department of Chemistry, School of Chemistry and Chemical Engineering, Northwestern Polytechnical University, Xi'an, Shaanxi 710072, China

Complete contact information is available at:

<https://pubs.acs.org/10.1021/acsomega.2c01412>

Notes

The authors declare no competing financial interest.

ACKNOWLEDGMENTS

This work was supported by the National Natural Science Foundation of China (No. 51433008), the Key Research Plan in Shaanxi Province of China (No. 2022GY-198), and Subject Construction Program of Northwestern Polytechnical University (No. 22GH010613). The authors are grateful for support from the High-Performance Computing Center, School of Chemistry and Chemical Engineering, and Office of Academic Affairs of Northwestern Polytechnical University.

REFERENCES

- (1) Knopman, D. S.; Amieva, H.; Petersen, R. C.; Chetelat, G.; Holtzman, D. M.; Hyman, B. T.; Nixon, R. A.; Jones, D. T. Alzheimer disease. *Nat. Rev. Dis. Primers*. **2021**, 7 (1), 33.
- (2) Hardy, J.; Selkoe, D. J. The amyloid hypothesis of Alzheimer's disease: Progress and problems on the road to therapeutics. *Science* **2002**, 297 (5580), 353–356.

- (3) Wang, C.; Yang, A.; Li, X.; Li, D.; Zhang, M.; Du, H.; Li, C.; Guo, Y.; Mao, X.; Dong, M.; et al. Observation of molecular inhibition and binding structures of amyloid peptides. *Nanoscale* **2012**, *4* (6), 1895–1909.
- (4) Zaman, M.; Khan, A. N.; Wahiduzzaman; Zakariya, S. M.; Khan, R. H. Protein misfolding, aggregation and mechanism of amyloid cytotoxicity: An overview and therapeutic strategies to inhibit aggregation. *Int. J. Biol. Macromol.* **2019**, *134*, 1022–1037.
- (5) Chen, S. Y.; Gao, Y.; Sun, J. Y.; Meng, X. L.; Yang, D.; Fan, L. H.; Xiang, L.; Wang, P. Traditional chinese medicine: Role in reducing β -amyloid, apoptosis, autophagy, neuroinflammation, oxidative stress, and mitochondrial dysfunction of Alzheimer's disease. *Front. Pharmacol.* **2020**, *11*, 497.
- (6) Cascella, M.; Bimonte, S.; Muzio, M. R.; Schiavone, V.; Cuomo, A. The efficacy of epigallocatechin-3-gallate (green tea) in the treatment of Alzheimer's disease: An overview of pre-clinical studies and translational perspectives in clinical practice. *Infect. Agent. Cancer* **2017**, *12* (1), 36.
- (7) Fusco, G.; Sanz-Hernandez, M.; Ruggeri, F. S.; Vendruscolo, M.; Dobson, C. M.; De Simone, A. Molecular determinants of the interaction of EGCG with ordered and disordered proteins. *Biopolymers* **2018**, *109* (10), e23117.
- (8) Harvey, B. S.; Musgrave, I. F.; Ohlsson, K. S.; Fransson, Å.; Smid, S. D. The green tea polyphenol (–)-epigallocatechin-3-gallate inhibits amyloid- β evoked fibril formation and neuronal cell death in vitro. *Food Chem.* **2011**, *129* (4), 1729–1736.
- (9) Visentin, C.; Pellistri, F.; Natalello, A.; Vertemara, J.; Bonanomi, M.; Gatta, E.; Penco, A.; Relini, A.; De Gioia, L.; Airolidi, C.; et al. Epigallocatechin-3-gallate and related phenol compounds redirect the amyloidogenic aggregation pathway of ataxin-3 towards non-toxic aggregates and prevent toxicity in neural cells and caenorhabditis elegans animal model. *Hum. Mol. Genet.* **2017**, *26* (17), 3271–3284.
- (10) Acharya, A.; Stockmann, J.; Beyer, L.; Rudack, T.; Nabers, A.; Gumbart, J. C.; Gerwert, K.; Batista, V. S. The effect of (–)-epigallocatechin-3-gallate on the amyloid- β secondary structure. *Biophys. J.* **2020**, *119* (2), 349–359.
- (11) Zhang, T.; Zhang, J.; Derreumaux, P.; Mu, Y. Molecular mechanism of the inhibition of EGCG on the Alzheimer $A\beta(1-42)$ dimer. *J. Phys. Chem. B* **2013**, *117* (15), 3993–4002.
- (12) Li, F.; Zhan, C.; Dong, X.; Wei, G. Molecular mechanisms of resveratrol and EGCG in the inhibition of $A\beta_{42}$ aggregation and disruption of $A\beta_{42}$ protofibril: Similarities and differences. *Phys. Chem. Chem. Phys.* **2021**, *23* (34), 18843–18854.
- (13) Zhan, C.; Chen, Y.; Tang, Y.; Wei, G. Green tea extracts EGCG and EGC display distinct mechanisms in disrupting $A\beta_{42}$ protofibril. *ACS Chem. Neurosci.* **2020**, *11* (12), 1841–1851.
- (14) Ding, J.; Xi, Y. D.; Zhang, D. D.; Zhao, X.; Liu, J. M.; Li, C. Q.; Han, J.; Xiao, R. Soybean isoflavone ameliorates β -amyloid 1–42-induced learning and memory deficit in rats by protecting synaptic structure and function. *Synapse* **2013**, *67* (12), 856–864.
- (15) Zaheer, K.; Humayoun Akhtar, M. An updated review of dietary isoflavones: Nutrition, processing, bioavailability and impacts on human health. *Crit. Rev. Food Sci. Nutr.* **2017**, *57* (6), 1280–1293.
- (16) Petry, F. D. S.; Hoppe, J. B.; Klein, C. P.; Dos Santos, B. G.; Hozer, R. M.; Bifi, F.; Matte, C.; Salbego, C. G.; Trindade, V. M. T. Genistein attenuates amyloid-beta-induced cognitive impairment in rats by modulation of hippocampal synaptotoxicity and hyperphosphorylation of tau. *J. Nutr. Biochem.* **2021**, *87*, 108525.
- (17) Devi, K. P.; Shanmuganathan, B.; Manayi, A.; Nabavi, S. F.; Nabavi, S. M. Molecular and therapeutic targets of genistein in Alzheimer's disease. *Mol. Neurobiol.* **2017**, *54* (9), 7028–7041.
- (18) Ma, W.; Ding, B.; Yu, H.; Yuan, L.; Xi, Y.; Xiao, R. Genistein alleviates β -amyloid-induced inflammatory damage through regulating Toll-like receptor 4/nuclear factor κ B. *J. Med. Food* **2015**, *18* (3), 273–279.
- (19) Petry, F. D. S.; Coelho, B. P.; Gaelzer, M. M.; Kreutz, F.; Guma, F.; Salbego, C. G.; Trindade, V. M. T. Genistein protects against amyloid-beta-induced toxicity in SH-SY5Y cells by regulation of Akt and Tau phosphorylation. *Phytother. Res.* **2020**, *34* (4), 796–807.
- (20) Ren, B.; Liu, Y.; Zhang, Y.; Cai, Y.; Gong, X.; Chang, Y.; Xu, L.; Zheng, J. Genistein: A dual inhibitor of both amyloid β and human islet amylin peptides. *ACS Chem. Neurosci.* **2018**, *9* (5), 1215–1224.
- (21) Khan, R. H.; Siddiqi, M. K.; Uversky, V. N.; Salahuddin, P. Molecular docking of $A\beta_{1-40}$ peptide and its Iowa D23N mutant using small molecule inhibitors: Possible mechanisms of $A\beta$ -peptide inhibition. *Int. J. Biol. Macromol.* **2019**, *127*, 250–270.
- (22) McDonald, I. K.; Thornton, J. M. Satisfying hydrogen bonding potential in proteins. *J. Mol. Biol.* **1994**, *238* (5), 777–793.
- (23) Doig, A. J.; Derreumaux, P. Inhibition of protein aggregation and amyloid formation by small molecules. *Curr. Opin. Struct. Biol.* **2015**, *30*, 50–56.
- (24) Han, B.; Liu, Y.; Ginzinger, S. W.; Wishart, D. S. SHITX2: Significantly improved protein chemical shift prediction. *J. Biomol. NMR* **2011**, *50* (1), 43–57.
- (25) Crescenzi, O.; Tomaselli, S.; Guerrini, R.; Salvadori, S.; D'Ursi, A. M.; Temussi, P. A.; Picone, D. Solution structure of the Alzheimer amyloid β -peptide (1–42) in an apolar microenvironment: Similarity with a virus fusion domain. *Eur. J. Biochem.* **2002**, *269* (22), 5642–5648.
- (26) Nguyen, P. H.; Derreumaux, P. Structures of the intrinsically disordered $A\beta$, tau and alpha-synuclein proteins in aqueous solution from computer simulations. *Biophys. Chem.* **2020**, *264*, 106421.
- (27) Hou, L.; Shao, H.; Zhang, Y.; Li, H.; Menon, N. K.; Neuhaus, E. B.; Brewer, J. M.; Byeon, I. J.; Ray, D. G.; Vitek, M. P.; et al. Solution NMR studies of the $A\beta(1-40)$ and $A\beta(1-42)$ peptides establish that the Met35 oxidation state affects the mechanism of amyloid formation. *J. Am. Chem. Soc.* **2004**, *126* (7), 1992–2005.
- (28) Gupta, S.; Dasmahapatra, A. K. Destabilization potential of phenolics on $A\beta$ fibrils: Mechanistic insights from molecular dynamics simulation. *Phys. Chem. Chem. Phys.* **2020**, *22* (35), 19643–19658.
- (29) Cerda-Costa, N.; Esteras-Chopo, A.; Aviles, F. X.; Serrano, L.; Villegas, V. Early kinetics of amyloid fibril formation reveals conformational reorganisation of initial aggregates. *J. Mol. Biol.* **2007**, *366* (4), 1351–1363.
- (30) Nguyen, P. H.; Li, M. S.; Derreumaux, P. Effects of all-atom force fields on amyloid oligomerization: Replica exchange molecular dynamics simulations of the $A\beta(16-22)$ dimer and trimer. *Phys. Chem. Chem. Phys.* **2011**, *13* (20), 9778–9788.
- (31) Liu, F. F.; Dong, X. Y.; He, L.; Middelberg, A. P.; Sun, Y. Molecular insight into conformational transition of amyloid β -peptide 42 inhibited by (–)-epigallocatechin-3-gallate probed by molecular simulations. *J. Phys. Chem. B* **2011**, *115* (41), 11879–11887.
- (32) Zhang, N.; Yeo, J. J.; Lim, Y. X.; Guan, P.; Zeng, K. Y.; Hu, X. L.; Cheng, Y. Tuning the structure of monomeric amyloid beta peptide by the curvature of carbon nanotubes. *Carbon* **2019**, *153*, 717–724.
- (33) Chen, H.; Zhang, Y.; Li, L.; Han, J. G. Probing ligand-binding modes and binding mechanisms of benzoxazole-based amide inhibitors with soluble epoxide hydrolase by molecular docking and molecular dynamics simulation. *J. Phys. Chem. B* **2012**, *116* (34), 10219–10233.
- (34) Hung, H. M.; Nguyen, M. T.; Tran, P. T.; Truong, V. K.; Chapman, J.; Quynh Anh, L. H.; Derreumaux, P.; Vu, V. V.; Ngo, S. T. Impact of the astaxanthin, betanin, and EGCG compounds on small oligomers of amyloid $A\beta_{40}$ peptide. *J. Chem. Inf. Model.* **2020**, *60* (3), 1399–1408.
- (35) Santuz, H.; Nguyen, P. H.; Sterpone, F.; Derreumaux, P. Small oligomers of $A\beta_{42}$ protein in the bulk solution with AlphaFold2. *ACS Chem. Neurosci.* **2022**, *13* (6), 711–713.
- (36) Morris, G. M.; Huey, R.; Lindstrom, W.; Sanner, M. F.; Belew, R. K.; Goodsell, D. S.; Olson, A. J. AutoDock4 and AutoDockTools4: Automated docking with selective receptor flexibility. *J. Comput. Chem.* **2009**, *30* (16), 2785–2791.
- (37) Frisch, M. J.; Trucks, G. W.; Schlegel, H. B.; Scuseria, G. E.; Robb, M. A.; Cheeseman, J. R.; Scalmani, G.; Barone, V.; Mennucci, B.; Petersson, G. A. *Gaussian 09W*, Revision A.02; Gaussian, Inc.: Wallingford, CT, 2009.

- (38) Malde, A. K.; Zuo, L.; Breeze, M.; Stroet, M.; Poger, D.; Nair, P. C.; Oostenbrink, C.; Mark, A. E. An Automated force field Topology Builder (ATB) and repository: Version 1.0. *J. Chem. Theory Comput.* **2011**, *7* (12), 4026–4037.
- (39) Volkamer, A.; Kuhn, D.; Grombacher, T.; Rippmann, F.; Rarey, M. Combining global and local measures for structure-based druggability predictions. *J. Chem. Inf. Model.* **2012**, *52* (2), 360–372.
- (40) Pettersen, E. F.; Goddard, T. D.; Huang, C. C.; Couch, G. S.; Greenblatt, D. M.; Meng, E. C.; Ferrin, T. E. UCSF Chimera-A visualization system for exploratory research and analysis. *J. Comput. Chem.* **2004**, *25* (13), 1605–1612.
- (41) Morris, G. M.; Goodsell, D. S.; Halliday, R. S.; Huey, R.; Hart, W. E.; Belew, R. K.; Olson, A. J. Automated docking using a Lamarckian genetic algorithm and an empirical binding free energy function. *J. Comput. Chem.* **1998**, *19* (14), 1639–1662.
- (42) Hou, X.; Du, J.; Zhang, J.; Du, L.; Fang, H.; Li, M. How to improve docking accuracy of AutoDock4.2: A case study using different electrostatic potentials. *J. Chem. Inf. Model.* **2013**, *53* (1), 188–200.
- (43) Huey, R.; Morris, G. M.; Olson, A. J.; Goodsell, D. S. A semiempirical free energy force field with charge-based desolvation. *J. Comput. Chem.* **2007**, *28* (6), 1145–1152.
- (44) Humphrey, W.; Dalke, A.; Schulten, K. VMD: Visual Molecular Dynamics. *J. Mol. Graph.* **1996**, *14* (1), 33–38.
- (45) Hess, B.; Kutzner, C.; van der Spoel, D.; Lindahl, E. GROMACS 4: Algorithms for highly efficient, load-balanced, and scalable molecular simulation. *J. Chem. Theory Comput.* **2008**, *4* (3), 435–447.
- (46) Schmid, N.; Eichenberger, A. P.; Choutko, A.; Riniker, S.; Winger, M.; Mark, A. E.; van Gunsteren, W. F. Definition and testing of the GROMOS force-field versions 54A7 and 54B7. *Eur. Biophys. J.* **2011**, *40* (7), 843–856.
- (47) Gerben, S. R.; Lemkul, J. A.; Brown, A. M.; Bevan, D. R. Comparing atomistic molecular mechanics force fields for a difficult target: A case study on the Alzheimer's amyloid β -peptide. *J. Biomol. Struct. Dyn.* **2014**, *32* (11), 1817–1832.
- (48) Berendsen, H. J. C.; Grigera, J. R.; Straatsma, T. P. The missing term in effective pair potentials. *J. Phys. Chem.* **1987**, *91* (24), 6269–6271.
- (49) Melchionna, S.; Ciccotti, G.; Holian, B. L. Hoover NPT dynamics for systems varying in shape and size. *Mol. Phys.* **1993**, *78* (3), 533–544.
- (50) Bussi, G.; Donadio, D.; Parrinello, M. Canonical sampling through velocity rescaling. *J. Chem. Phys.* **2007**, *126* (1), 014101.
- (51) Nose, S.; Klein, M. L. Constant pressure molecular dynamics for molecular systems. *Mol. Phys.* **1983**, *50* (5), 1055–1076.
- (52) Hess, B.; Bekker, H.; Berendsen, H. J. C.; Fraaije, J. G. E. M. LINCS: A linear constraint solver for molecular simulations. *J. Comput. Chem.* **1997**, *18* (12), 1463–1472.
- (53) Darden, T.; York, D.; Pedersen, L. Particle mesh Ewald: An $N \log(N)$ method for Ewald sums in large systems. *J. Chem. Phys.* **1993**, *98* (12), 10089–10092.
- (54) Abraham, M. J.; Murtola, T.; Schulz, R.; Páll, S.; Smith, J. C.; Hess, B.; Lindahl, E. GROMACS: High performance molecular simulations through multi-level parallelism from laptops to supercomputers. *SoftwareX* **2015**, *1–2*, 19–25.
- (55) Nguyen, P. H.; Ramamoorthy, A.; Sahoo, B. R.; Zheng, J.; Faller, P.; Straub, J. E.; Dominguez, L.; Shea, J. E.; Dokholyan, N. V.; De Simone, A.; et al. Amyloid oligomers: A joint experimental/computational perspective on Alzheimer's disease, Parkinson's disease, type II diabetes, and amyotrophic lateral sclerosis. *Chem. Rev.* **2021**, *121* (4), 2545–2647.
- (56) Frishman, D.; Argos, P. Knowledge-based protein secondary structure assignment. *Proteins* **1995**, *23* (4), 566–579.
- (57) Hooft, R. W.; Sander, C.; Scharf, M.; Vriend, G. The PDBFINDER database: A summary of PDB, DSSP and HSSP information with added value. *Comput. Appl. Biosci.* **1996**, *12* (6), 525–529.
- (58) Kumari, R.; Kumar, R.; Open Source Drug Discovery, C.; Lynn, A. g_mmpbsa-A GROMACS tool for high-throughput MM-PBSA calculations. *J. Chem. Inf. Model.* **2014**, *54* (7), 1951–1962.
- (59) Homeyer, N.; Gohlke, H. Free energy calculations by the Molecular Mechanics Poisson-Boltzmann Surface Area method. *Mol. Inform.* **2012**, *31* (2), 114–122.